Field tests to assess the effectiveness of ground improvement for liquefaction mitigation

A. Flora, A. Chiaradonna, E. Bilotta, G. Fasano & L. Mele
DICEA, University of Napoli Federico II, Italy

S. Lirer
DIS, Marconi University, Roma, Italy

L. Pingue, F. Fanti
TREVI Ltd.,Cesena, Italy

ABSTRACT: One of the main goals of the LIQUEFACT project is the analysis of the effectiveness of some ground improvement techniques in the mitigation of seismically induced soil liquefaction risk. This aspect was addressed via a comprehensive experimental program by means of laboratory and centrifuge tests, as well as by carrying out a number of tests in a field trial located in Pieve di Cento (Italy), where a shaker was placed at ground level to generate cyclic shear stresses at ground level to induce a significant build-up of pore pressure in the shallow liquefiable sandy layer. Three series of tests were carried out: one in a zone without treatments (UN), one in a zone where horizontal drains (HD) were installed in the liquefiable layer, and one in a zone in which air was insufflated through sub horizontal pipes to partially desaturate the liquefiable soil (induced partial saturation, IPS). The paper describes in some detail the test layout and reports the results obtained during some of the tests carried out. The vibrator was able to generate high pore pressure build-up in the untreated zone, locally inducing liquefaction in one of the tests. IPS was extremely effective in reducing pore pressure increments during shaking, with values close to zero. This confirms the potential of this innovative liquefaction mitigation technology.

1 INTRODUCTION

Liquefaction is a phenomenon that may take place in loose saturated sandy deposits subjected to earthquake shaking. This mechanism is associated with a sharp decrease in soil strength and stiffness caused by the pore water pressure increments induced by the dynamic action.

Soil liquefaction can cause serious damage to engineering structures and, as a consequence, many types of mitigation techniques (densification, drainage, addition of fines, etc.) have been developed in time. The H2020 LIQUEFACT project aims among other goals to assess the effectiveness of some innovative mitigation techniques. Among these, horizontal drains (HD) and induced partial saturation (IPS) were chosen in the project. Laboratory and centrifuge tests were carried out to test the effectiveness of both techniques (Fasano et al. 2018, Fioravante et al. 2019, Mele et al. 2018, 2019, De Sarno et al. 2019, Lirer et al. 2019) and numerical simulations were performed to extend the experimental results. It was demonstrated (Fasano et al. 2018, Fioravante et al. 2019; Mele et al. 2018, 2019, De Sarno et al. 2019) that both HD and IPS are effective as mitigation techniques in reducing pore pressure increments during dynamic shaking, consistently with the available literature. Then, a field trial was programmed to confirm these conclusions at a real scale. Liquefaction field trials are very difficult to implement, and few examples are available in literature. Two alternative approaches can be adopted: soil blasting (Amoroso et al. 2018) or shaking from ground level to induce high deformations in the soil (van Ballegooy et al. 2015). In the LIQUEFACT project, the second choice was taken for a number of reasons, the most important one being the fact that the field trial site was too close to some buildings to allow explosives to be used. This paper reports some of the results obtained in the trial tests, along with some preliminary considerations.

2 TEST SITE GEOTECHNICAL CHARACTERIZATION

The chosen test site is located in the Pieve di Cento municipality (Emilia Romagna Region), in the Po valley, where the 2012 Emilia seismic sequence (M_L=5.9 and M_L=5.8 on May 20 and 29 respectively) produced significant and widespread liquefaction effects (Figure 1a). The site is close to a paleochannel of the Reno river, and the subsoil is made of loose alluvial deposits. The field trial was conceived to compare the pore pressure build-up in shallow sandy soils without and with mitigation techniques against liquefaction, generating a dynamic shaking action at ground level. As explained in more detail in §3, two innovative mitigation actions were tested: horizontal drainage (HD) and induced partial saturation (IPS). In order to have a detailed knowledge of local subsoil conditions, in-situ geotechnical testing was concentrated in the areas where the two mitigation techniques were installed (Figure 1b).

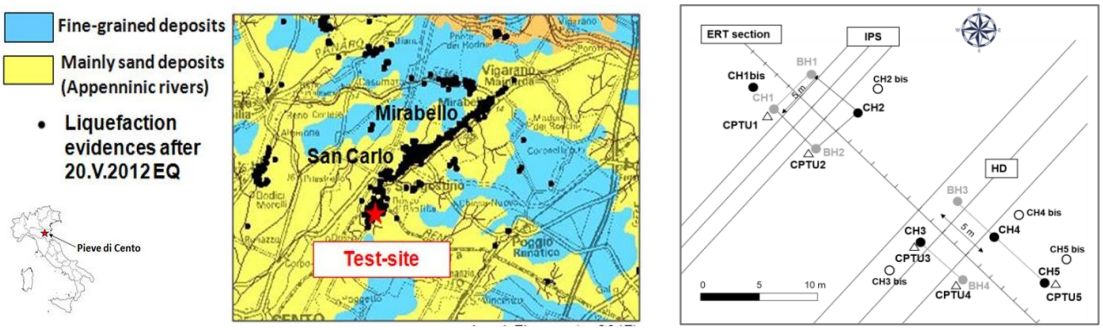

(a) (b)

Figure 1. (a): Location of the test site (red star) and evidences of liquefaction (black dots) in the area during the 2012 Emilia sequence (Giretti & Fioravante 2017); (b) plan of test site.

Ground investigation consisted of:

- 14 boreholes to a depth of 10 m, retrieving undisturbed samples (Osterberg and Gel Push);
- 5 CPTU to a depth of 11 m;
- Cross-Hole tests and V_p tomographies (the latter along the alignments CH2-BH2-CH1-BH1-CH2, CH3-BH4 and BH3-CH4-CH5);
- Electric Resistivity Tomographies (ERT) in the same boreholes used for the Cross-Holes;
- An Electrical Resistivity Tomography (ERT) using a surface array as sketched in Figure 1b.

Based on all the information gained from the in situ and laboratory investigation, the soil profile reported in Figure 2a was obtained. Figure 2b shows the soil behaviour type index I_c (Robertson 2009) obtained from the interpretation of the CPTUs: the values of $I_c(z)$ are similar along the different verticals, indicating that in the investigated area the subsoil layering can be considered horizontal. In particular, soil stratigraphy consists of an upper crust (1.0 m thick) of silty sand, overlying a sandy silt layer of about 1.8 m. A grey silty sand layer (GSS) is located between 2.8 and 6 m, with an intermediate thin clayey layer (continuous, at least in the investigated area) at a depth between 4.4 and 4.7 m. Below 6 m, a thick silty clayey deposit is found to the maximum investigated depth. From the grading point of view, the sandy silty layer (SS) is heterogeneous (well-graded and with a low plasticity fine content variable in the range 60 – 85%), while the grey silty sand (GSS) is more homogeneous, with a fine content ranging from 5% to 12 %. The clayey layer can be assumed as an impermeable lower boundary for the problem under investigation. The ground water table is at 1.8 m below the ground level.

The liquefaction susceptibility analyses indicate that the grey silty sand (GSS) is the liquefiable layer. This is consistent with its loose state ($D_r \approx 40\%$, $V_s \approx 130$ m/s), full saturation, low stress level and a soil behaviour type index I_c on average lower than 2.0 (Figure 2b). For such a reason, the two mitigation techniques (HD and IPS) were installed in the upper GSS layer, the shallowest liquefiable layer.

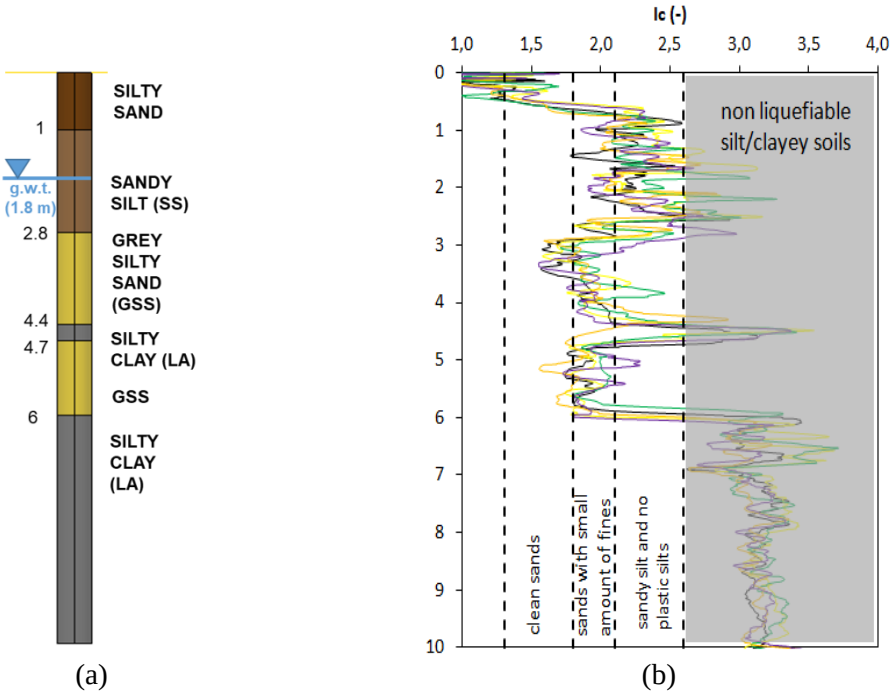

(a) (b)

Figure 2. (a) Representative soil profile, from both in situ and lab tests; (b) soil behaviour type index I_c.

3 MITIGATION TECHNIQUES: DESCRIPTION AND INSTALLATION

The HD system was installed using patented high porosity polyethylene micropored well screens, having an external diameter of 180 mm and a thickness of 15 mm. Two different geometrical configurations were adopted (Fig. 3a):

- a linear configuration, in which three draining pipes were located at the constant depth of 3.5 m from the original ground level with a spacing of 1.8 m;
- a rhomboidal configuration: four draining pipes located at the depths of 2.8 m, 3.5 m and 4.2 m from the original ground level, with a spacing of 1.0 m.

In order to reduce soil disturbance to a minimum, the adopted procedure of installation was:

1. 78 m long "U" shaped directional drilling with a slant drill bit (Ø 76 mm), to make sure that a sub horizontal central part of the pipes was placed at the desired depth;
2. rods' withdrawal by reaming the hole with a swivel device;
3. installation of the welded polyethylene pipes (Ø 180 mm) along the whole drilled length (78m); in particular, the central part of the pipes (18 m, placed below the testing area) is draining, while the two sides (30 m each) are blind.

For the IPS system, the partial saturation of the soil below the ground water table was obtained by injecting pressurized air from four sub horizontal pipes (with external diameter of 75 mm) placed in two rows at the depths of 3.0 and 4.0 m (Fig. 3b) from the original ground level, with a horizontal spacing of 2 m. The air was pumped into the pipes at a pressure high enough to win water hydrostatic pressure, but not so high to generate soil displacement or erosion (p=30 kPa for the shallowest pipes and 40 kPa for the deepest alignment). The IPS pipes were installed with a procedure simpler than for the HD system because of a significantly lower lateral friction of pipes:

1. 78 m long "U" shaped directional drilling with a sliced cutter (Ø 76 mm), to make sure that a sub horizontal central part of the pipes was placed at the desired depth;
2. rods' withdrawal by reaming the hole with a swivel device and simultaneous dragging of the welded polyethylene pipes (Ø 75 mm) along the whole drilled length (78 m); the central part of the pipes (18 m, placed below the testing area) is micropored (thus allowing air injection), while the two sides (30 m each) are blind. During air injection, packers were used to isolate a central draining length of just 10 m.

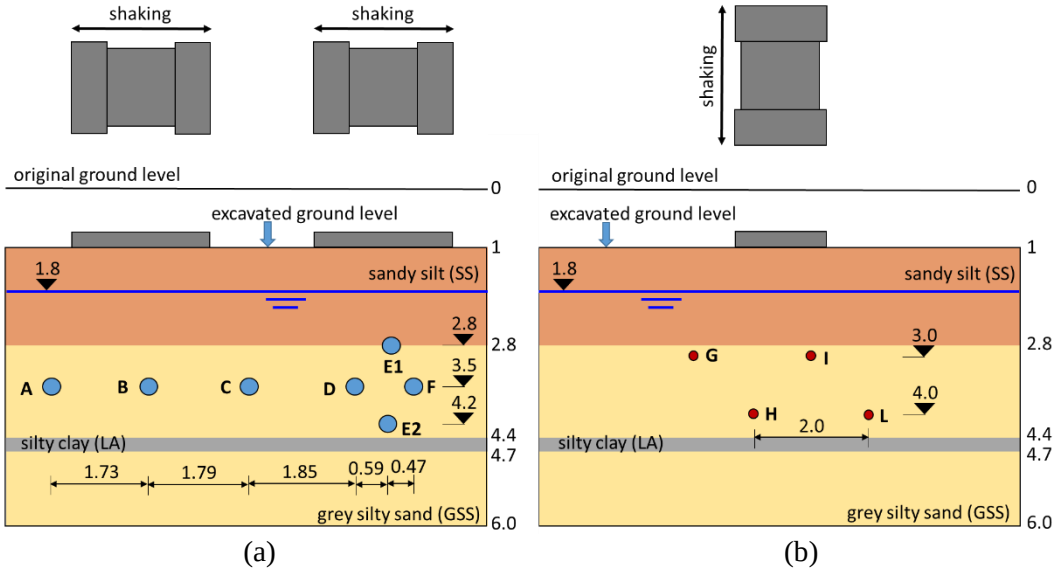

Figure 3. Geometrical schemes of the cross sections on (a) HD pipes and (b) IPS pipes.

Reamers with a diameter exceeding by just 10% the pipes' diameter were used for both HD and IPS, and a low viscosity natural biodegradable polymer slurry was adopted as drilling fluid to reduce soil disturbance to a minimum. Because of this, no settlement was observed at ground level during installation. This is an important technical detail in case these technologies have to be adopted in real liquefaction mitigation jobs, close existing structures.

For the IPS system, some preliminary in situ air injection tests were performed in July 2018, in order to calibrate the testing procedure. The theoretical values of the degree of saturation S_r for different values of the volume of injected air, V_a, are reported in Figure 4. Making reasonable assumptions on the extension of the treated soil volume in terms of length (10 m between the packers) and width (4 m), V_a is calculated for two possible heights: h=2.2 m (Fig. 4a), i.e., the air bubbles diffuse in all the volume of soil up to the ground water table; h=1.2 m (Fig. 4b), i.e., the air bubbles diffuse only in the GSS layer, assuming that the upper sandy silt is fine enough to avoid significant air entrance. As will be shown later commenting Cross-Hole and ERT results, the first hypothesis (h=2.2 m) is the more realistic one, hence reference will be done to Figure 4a.

Since some air was lost in a visible way through the boreholes still open (bubbling at ground level was observed), and some air likely left the treated volume through the water table as well, in the Figure 4 different curves are reported for different values of such a lost volume of air. Whatever the percentage of air lost, the final value of S_r after the injection of 15 m^3 of air should be not higher than 90-93%, a value low enough to guarantee a relevant increase of the cyclic resistance of the GSS layer (Mele et al. 2018).

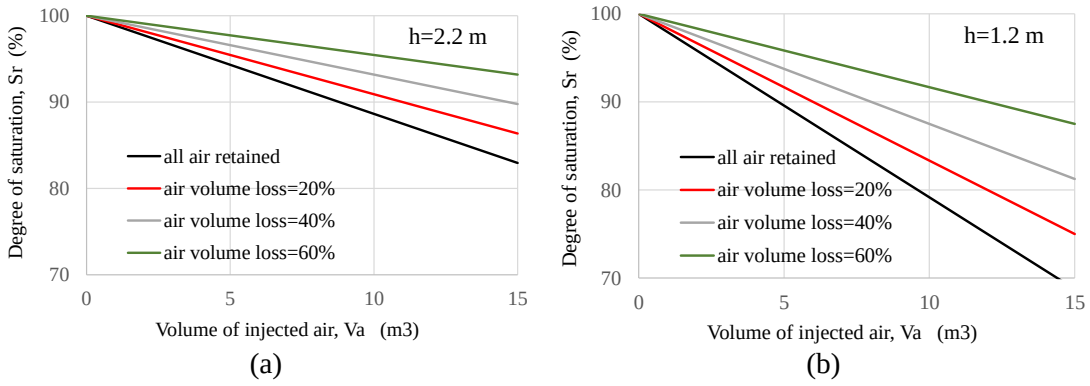

Figure 4. Theoretical values of S_r in the volume of GSS treated with IPS: (a) h=2.2 m, (b) h=1.2 m.

Cross-Hole tests and ERT were carried out to check the effect of air injection, respectively measuring the velocity, V_P, of compression waves and the soil resistivity, ρ, both sensitive to a change in the saturation degree.

Figure 5a and 5b report respectively the S_r-V_p and the S_r-ρ experimental relationships for the GSS obtained in small models in the laboratory (at a temperature of 22 °C), used to interpret the in situ testing results relating the measurements of V_p and ρ to values of S_r.

There is still some arguing in the academic community on the most effective way to measure the degree of saturation on site. For the V_p measurement, the main criticisms refer to two issues: the first is that the relationship between the degree of saturation, S_r, and the velocity V_p depends on the size of the air bubbles, and such a size depends on both the injection and surrounding water pressures (Tamura et al. 2002); the second, and more important, is that the S_r-V_p relationship has usually a sharp drop in the range $99\%<S_r<100\%$ (as confirmed by Fig. 5a), reaching a plateau for lower values of S_r that makes the interpretation of V_p uncertain. Furthermore, desaturation reduces the P-waves velocity so much that the risk of misinterpreting the results is very high in this case: in fact, the high ratio of V_p between the untreated and treated soil volumes makes it possible for the reflected head waves to be the first ones read by the receiver. In other words, the fastest P-waves may not be the ones travelling on the shortest length, and the apparent velocity $V_{p,a}$ may be just meaningless. ERTs present less criticalities, but they are less common and less sensitive to small variations in the range of extremely high degrees of saturation. Because of this, the two testing technologies may be seen as complementary.

During the injection calibration tests (July 2018), the Cross-Hole and ER tests were carried out after the injection of 1 m^3, 5 m^3 and 15 m^3 of air into the soil. Figures 6 and 7 report the results before and after IPS. Figure 6, in particular, reports the ERT tomographies, showing that before air injection the average value of ρ in the GSS layer (2.8-4.4 m depth) was about 36 Ohm·m in the central part, consistently with the value obtained in laboratory for S_r=100% (Fig. 5b) in the same soil. Higher values were detected close to the boreholes from which the measurements were done. Upon treatment with 5 m^3 of air, as expected the resistivity has a more random distribution, with values in the central part of the GSS layer ranging between 40 and 50 Ohm·m, with an average value of about 44. According to Fig. 5b, for the GSS layer this result corresponds to the range $93\%<S_r<100\%$, with an average value of 96%. Such a value is consistent with the theoretical expectation (Fig. 4) if the volume of air lost is no more than 20% of the injected amount. The ERT tomography after injecting 15 m^3 of air is not reported in the paper, because the interpretation is still under course. The difficulty in interpretation depends on the high variability of ρ in the investigated volume of soil, likely because of the non-uniform distribution of the air bubbles.

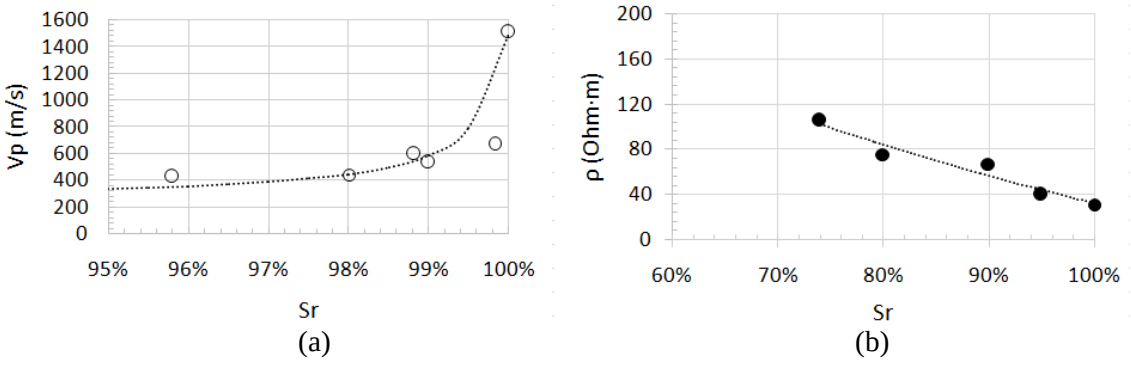

Figure 5. Experimental relationship between S_r and (a) V_p and (b) ρ for the GSS measured in laboratory in a small-scale model at a low confining pressure.

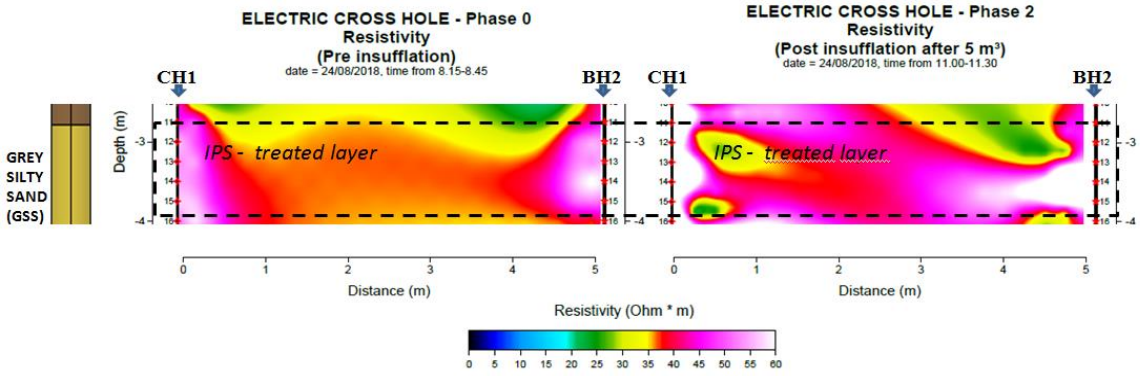

(a) (b)

Figure 6. Detail of the spatial distribution of electric resistivity (result of ERT) along the section CH1-BH2 before air injection (a) and after the injection of 5 m^3 of air (b) for the layer of grey silty sand (GSS).

Figure 7 reports the results of the Cross-Hole tests before air injection and after the injection of 15 m^3. The reduction of V_p in the GSS layer to a minimum value close to 950 m/s would correspond to a degree of saturation higher than 99% (Fig. 5a), which is in contradiction with the volume of air injected and with the ERT results. Likely, the head P-waves at the saturated-unsaturated interface were faster than the ones travelling in the unsaturated soil (as confirmed by back calculations), and thus the values of V_p reported in Figure 7 are apparent and not real, because they were obtained with a misinterpretation of the signal.

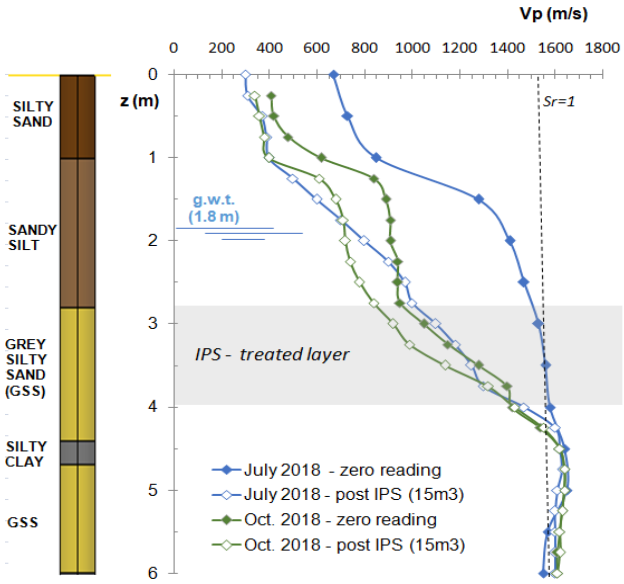

Figure 7. Apparent P-waves velocity V_p profile measured before and after the preliminary air injection tests (July 2018), and before and after the field trial tests (October 2018).

The apparent values of V_p calculated after 3 months (October 2018), before and after the new insufflation of air, kept the same values in the GSS layer. Since some increase of S_r likely took place between July and September 2018, and a subsequent decrease was certainly induced by air insufflation, this is a confirmation of the fact that the values of V_p reported in Figure 7 are apparent and not real. In all cases, in fact, the measured arrival times are those of the reflected head P-waves. As a consequence, in this specific case the results of ERT can be considered much more reliable. It can be argued that in the case of higher thicknesses of IPS treated volumes, V_p measurements can be still of interest to check the value of S_r, provided the distance between the boreholes is carefully taken as small as possible.

4 FIELD TESTS LAYOUT AND SEQUENCE

The goal of the field tests was the comparison of the liquefaction potential of the in-situ soil with and without the two selected mitigation techniques (HD and IPS). A shear-wave vibrator (M13S/609 S-Wave, Fig. 8) was used as a dynamic loading source at the ground surface. The shaker has two base plates with a saw tooth surface to ensure a good coupling with the base soil. The plates are pushed vertically to the fixed vertical load before shaking. A preliminary 1 m deep excavation was realized in all the field trial area in order to place the dynamic loading source closer to the liquefiable GSS deposit. A thin layer of gravel was placed at the ground surface in order to facilitate machine movement, having the attention of leaving without gravel the base plates – soil interface surfaces.

In each test, the static vertical loading of the shaker was first applied and, after waiting for consolidation via the check of pore pressure increments dissipation in the subsoil, the dynamic loading was applied, for a duration ranging between 100 s and 200 s. Since the vibrator generates in plane cyclic movements of the base plates, pure shear waves are generated into the subsoil only if the machine is perfectly horizontal and keeps this position; in the case (as it happened during all tests) of an irregular settlement of the machine, some tilting occurs and therefore the shaking generates both horizontal shear and vertical compression waves.

Pore pressure transducers (with high air entry value porous stones, previously saturated with silicon oil) and geophones were installed in the subsoil below the loading areas to monitor soil response to shaking (Fig. 9b). A detailed topographic and photogrammetric survey was also carried out in order to measure the ground settlements during the tests.

Figure 9a shows the four areas where the liquefaction tests were carried out. In Area 1 (untreated area) some tests were performed to analyze the response of the untreated soil to shaking. In Areas 2 and 3, tests were performed to verify the effectiveness of horizontal drainage HD ("rhomboidal configuration" in Area 2 and "linear configuration" in Area 3, see Fig. 3). Finally, in Area 4, the liquefaction tests were carried out to analyze the response of the soil treated with IPS. The in-situ tests were carried out in the four areas with the following steps:

1. application of the self-weight of the shaker (static vertical load);
2. waiting for the completion of the subsequent consolidation process;
3. shaking (duration of 100 s or 200 s, frequency of 10 Hz or 5 Hz);
4. monitoring dissipation of the excess pore pressure induced in the step 3 up to stabilization.

Table 1 reports the list of all the executed tests. In all the tests, large settlements of the loading plates took place during shaking. As reported in the notes of Table 1, such displacements were not uniform, and therefore the plates tilted during the tests. In some cases, large settlements and tilting brought the test to a stop before the programmed end, with the vertical loading pistons reaching their full span. In all cases, the settlements of plates were large and they took place with a local punching mechanism (Fig. 10), with basically no settlements outside the area directly loaded by the plates. Because of this, the soil was highly densified immediately below the shaker, becoming much stiffer. Then, subsequent shakings on the same area gave different excitations to the GSS layer, being the transmission of energy more efficient.

(a)

Type	**M13S/609 S-WAVE**
Maker	Mertz Inc
Hold Down Weight	178 kN
Reaction mass	3175 kg
Base plate	0.6 x 1.6 m
Peak force	138 kN
Frequency range	3 – 80 Hz

(b)

Figure 8. The adopted shaker, with a detail of one of the shaking base plates; (b) main features of machine.

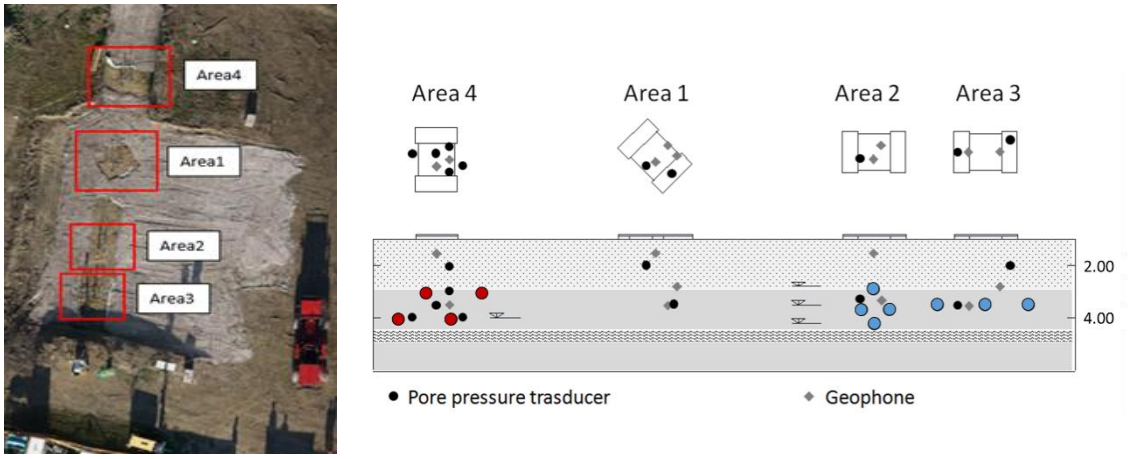

(a) (b)

Figure 9. (a): Air view of the testing areas; (b) cross section of the four testing areas: Area 1=untreated area; Area 2=rhomboidal configuration of the horizontal drains (HDR); Area 3= linear configuration of the horizontal drains (HDL); Area 4=induced partial saturation (IPS).

The horizontal input acceleration imposed by the vibrator was recorded with an accelerometer located on one of the base plates. Figure 11 reports an example of registration in one of the tests with a frequency of 10 Hz (average value of a_{max}=2 g). In all tests with this frequency, the input motion was the same.

Table 1. List of all the tests carried out in the Pieve di Cento field trial,

ID	Date	Mitigation technique	Frequency, f (Hz)	Duration, Δt (s)	Notes
UN_1	22/10/2018	UN	10	100	-
UN_2			10	100+100	Large tilting of the shaker
UN_3			5	100	-
UN_4	23/10/2018		10	100	Gravel layer introduced
UN_5			10	100	Gravel layer introduced
HDL_1	22/10/2018	HDL	10	100	-
HDL_2			10	100+100	-
HDR_1		HDR	10	100	-
HDR_2			10	100+100	-
IPS_1	23/10/2018	IPS	10	100	-
IPS_2			10	100+100	Stop after 100 s (large tilting)
IPS_3			5	100	-

UN=untreated area, HDL= single row of horizontal drains, HDR= four drains with a rhomboidal layout, IPS=induced partial saturation. The frequency and duration refer to the shaking imposed by the vibrator.

(a) (b)

Figure 10. Details of a plate, tests UN (Area 1): (a) plate cross section (blue dotted line), soil profile close to plate showing punching (red line), average settlement (in white); (b) loading plate upon retrieval.

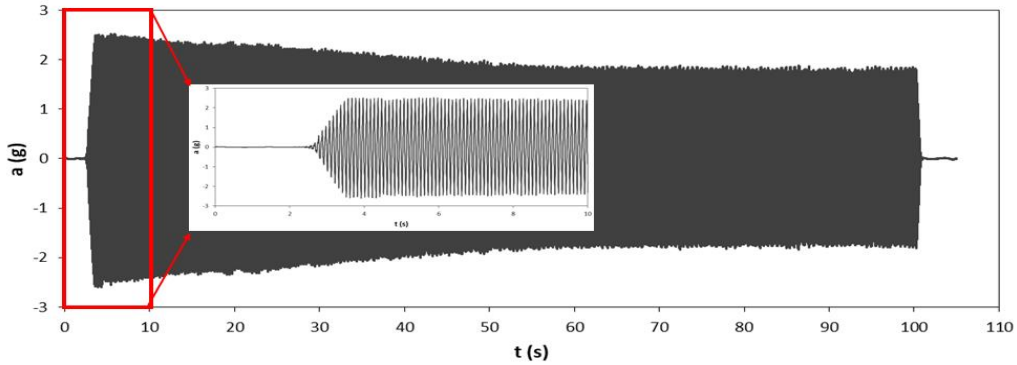

Figure 11. Input signal recorded on one of the base plates of the vibrator, for a test at f=10 Hz.

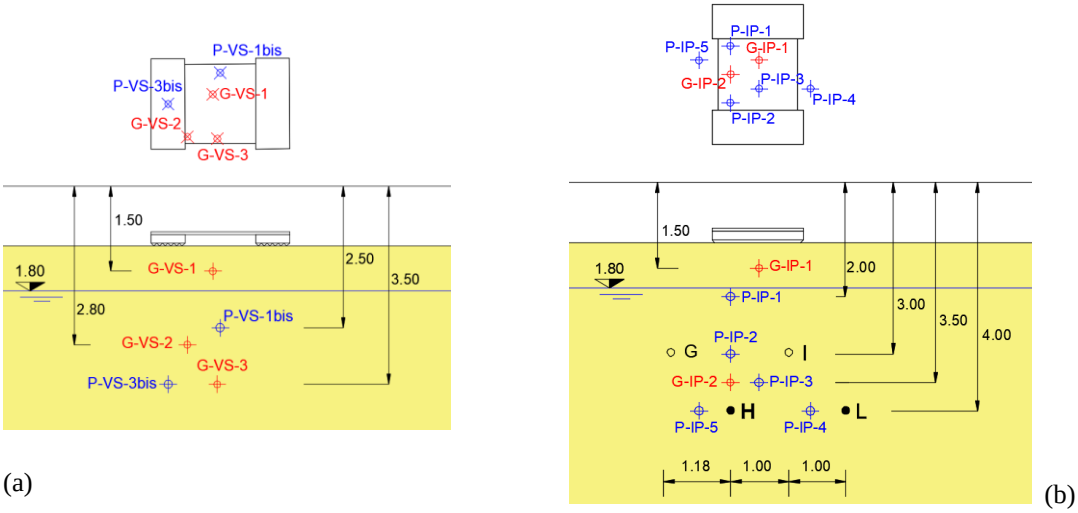

(a) (b)

Figure 12. Position of pressure transducers (P) and 2D geophones (G): (a) in the untreated area (Area 1); (b) in the area treated with IPS (Area 4). The air injection pipes are represented by empty circles (pipes G and I) and black circles (pipes H and L). During the field trial air was injected only through pipes H and L.

5 SOME FIELD TESTS RESULTS

5.1 *Results in the untreated zone (Area 1)*

In Area 1, two pore pressure transducers (P) and three 2D geophones (G) (measuring the vertical component and the horizontal one, in the direction of the applied shaking, of velocity) were placed into the soil at different depths (z) from the vibrating source (Fig. 12a). In this paper, for the sake of brevity only the results obtained in tests UN_1 and UN_2 will be analyzed. A close up of the first half second of recording of the geophones for tests UN_1 is reported in Figure 13: Figure 13a clearly shows the large values of the horizontal component of velocity registered by the upper geophone (G-VS-1), and the sharp reduction registered in the deeper ones, further from the shaking source. As previously mentioned, the motion applied at ground level also generated a vertical cyclic component of action in all tests (Figure 13b).

The ability of the vibrator to generate a strong excitation in the soil is confirmed by the high values of the mean shear strains computed in the subsoil respectively between the two geophones G-VS-1 and G-VS-2 (γ_{12}) and between the two geophones G-VS-2 and G-VS-3 (γ_{23}). Such shear strains are indicated for both tests UN_1 and UN_2 in Figure 14 in a plot showing the result of a torsional shear (TS) test on the Pieve di Cento grey sand (GSS): γ_{12} is always significantly higher than the volumetric-distortional coupling values (in particular, for the test UN_2), confirming the ability of the adopted means to generate pore pressure increments in the soil. The results of test UN_1 are summarized in Figure 15, in terms of the pore pressure ratio r_u time histories (where r_u is the ratio $\Delta u/\sigma'_v$ between the measured pore pressure increments and the effective vertical stress, computed considering the self-weight of the shaker) and acceleration time histories.

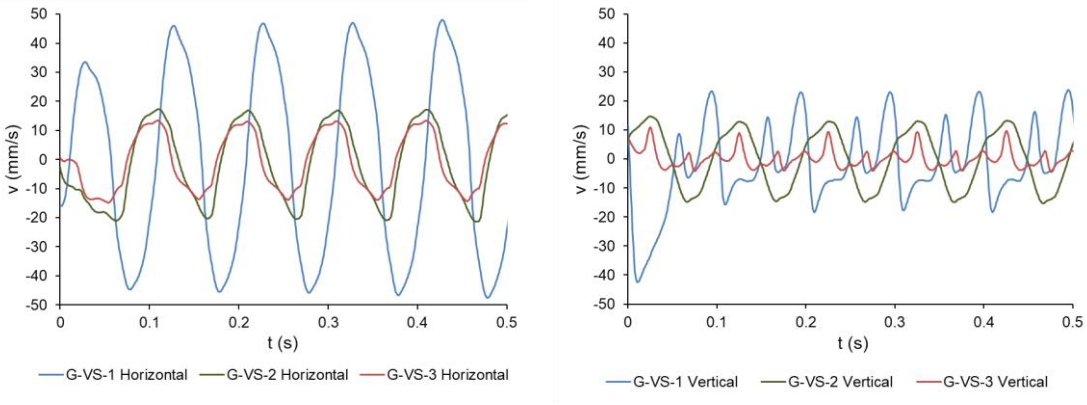

(a) (b)

Figure 13. Close up of the horizontal (a) and vertical (b) components of the velocities measured in the first 0.5 seconds from the geophones in Area 1.

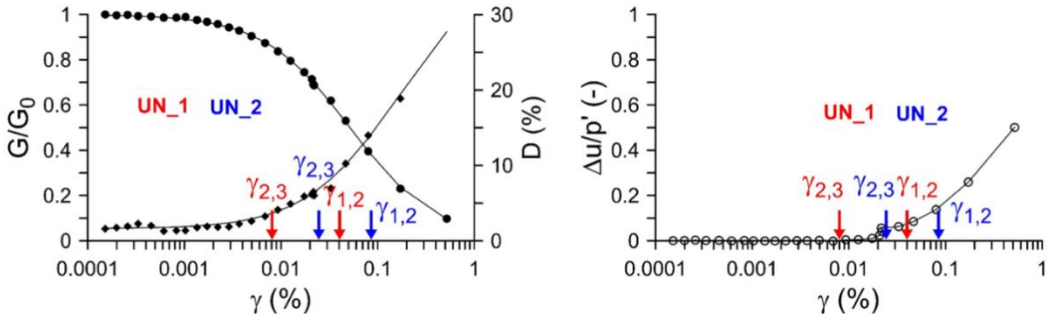

Figure 14. Results of TS test on the Pieve di Cento grey silty sand (GSS) along with some results from experiments UN_1 and UN_2 (see Tab. 1): the red and blue arrows indicate the average shear strains measured respectively during test UN_1 and UN_2 between the geophones G-VS-1 and G-VS-2 (γ_{12}) and between the geophones G-VS-2 and G-VS-3 (γ_{23}).

As obvious, the highest values of r_u pertain to the most superficial pressure transducer. Because of the relatively high coefficient of consolidation of the GSS and of the localized ground motion, relatively quick three-dimensional consolidation was expected. As a consequence, after a relatively short fully undrained phase of shaking, the measured pore pressure increments were certainly affected by a partial drainage. The time histories of r_u reported in Figure 15 seem to confirm this qualitative observation. Notwithstanding the partial drainage, values of r_u as high as 0.5 were measured. In this test, the average vertical displacement of the vibrating plates was 9 cm. Figure 16 reports the results obtained in test UN_2 for the first 100 seconds. In this case, because of the settlement induced by test UN_1, higher energies were transmitted to the GSS layer through the densified soil, as shown by the higher values of both the horizontal and vertical acceleration components. As a consequence, higher pore pressure increments were recorded. The upper pore pressure transducer indicates that liquefaction ($r_u \geq 0.9$) was locally induced. The r_u time history of the deeper pressure transducer (P-VS-3bis) reported in Figure 16 confirms that drainage started after few seconds, and a complex flow pattern was certainly taking place in the volume of soil affected by the shaking. Sand ejecta were observed immediately around the shaking plates.

During this test, very large settlements of the loading plate were measured, with a continuously increasing tilting of the shaker. The average final vertical displacement of the vibrating plates was in this test 32 cm, which brought the pistons loading the shaking plates to reach their full span before the programmed end of the test.

5.2 *Results in the zone treated with IPS (Area 4)*

In this area, five pore pressure transducers (P) and two 2D geophones (G) were placed into the soil at different depths (z) from the vibrating source (Figure 12b). Since the tests were carried out

about two months after the first insufflation of air in the subsoil (see §3), before restarting insufflation a zero reading of V_p was done (Fig. 7). The values of the apparent velocity V_p were still well below those corresponding to full saturation, with only a minor increase of V_p in the shallowest part of the subsoil. As previously mentioned, being the values reported in Figure 7 referred to apparent velocities, they did not give any precise indication on the degree of saturation, confirming only that most of the air previously injected into the soil was still trapped there.

However, a new injection of air was performed, keeping a constant air flow. The tests in this area were carried out after a time long enough to inject 15 m^3 of air, from the same length of tubes (10 m). In this case the whole flow was injected only through the two lower pipes (Fig. 12b), since the air injected by the upper two would have likely moved upwards, out of the liquefiable silty sand. Assuming that only 20% of the insufflated air was lost, the sum of the newly injected volume of air to that injected to the calibration test would lead to very low degrees of saturation (as low as S_r=60%). However, the available information is insufficient to give a value of the final value of S_r. The final values of $V_p(z)$ are not reported in the figure because are of no help, being in all similar to the ones measured immediately after the calibration tests carried out three months before. Again, this is a further confirmation of the fact that the values of V_p reported in the figure are apparent and not real. The experimental results obtained in test IPS_1 are summarized in figure 17. The accelerations calculated on the measurements of the G-IP-2 geophones are not shown in the figure because this instrument did not work properly. In this case, IPS showed to be extremely effective: the pore pressure increments during shaking were so small to be negligible (Δu<2 kPa, $r_{u,max}$=0.07), and a much stiffer behaviour could be observed on site, with no fluid sand ejecta and no water outcome.

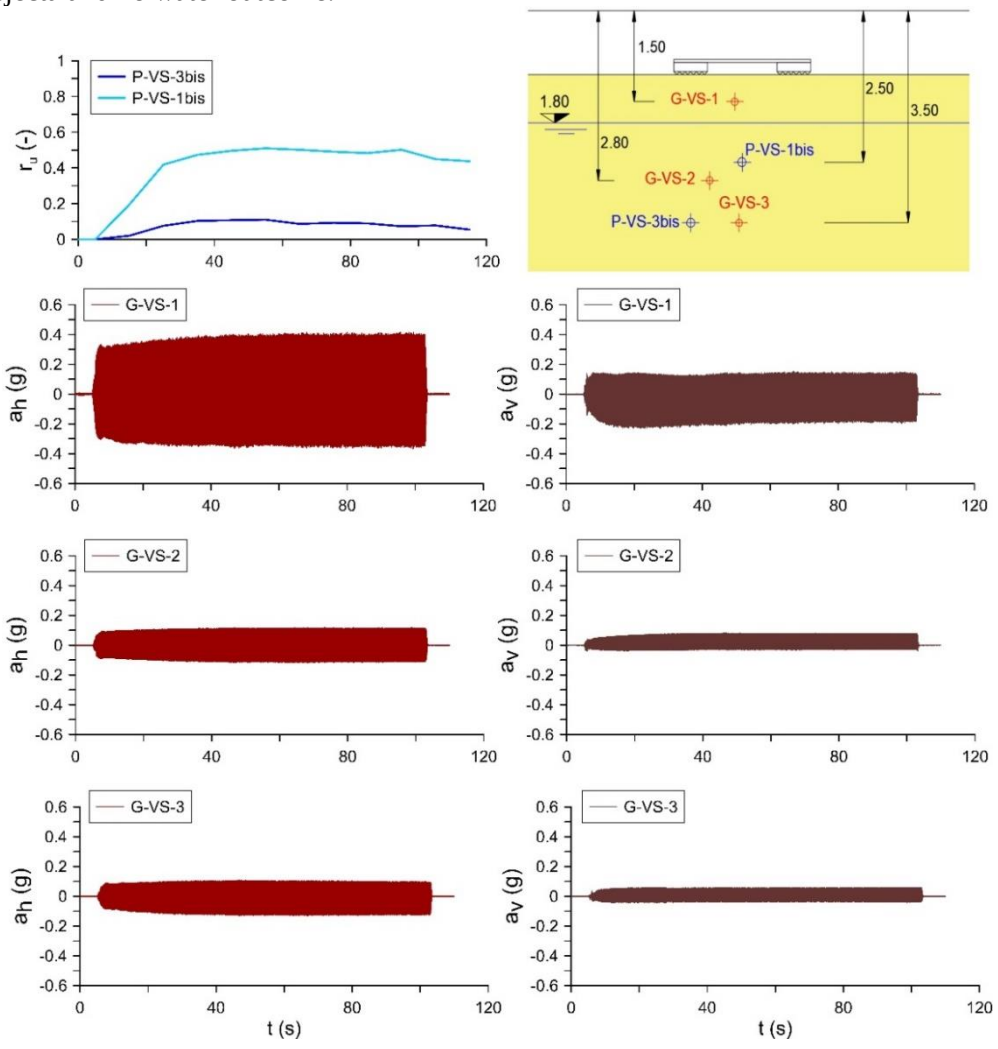

Figure 15. Results of test UN_1. Time histories of the pore pressure increment ratio r_u and of the horizontal, a_h, and vertical, a_v, components of acceleration in the three geophones G-VS-1, G-VS-2 and G-VS-3.

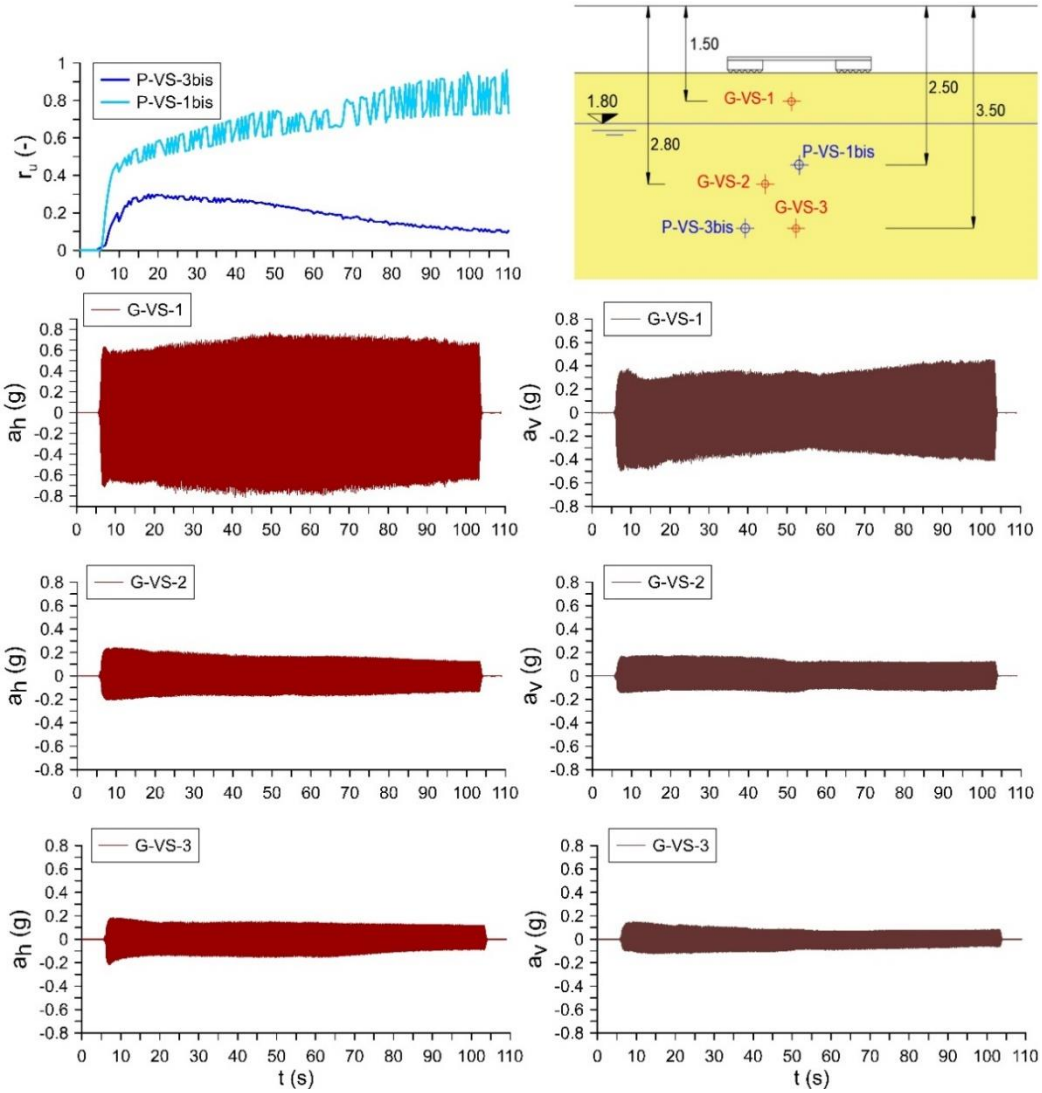

Figure 16. Results of test UN_2. Time histories of: pore pressure ratio r_u; horizontal, a_h, and vertical, a_v, components of acceleration in the three geophones G-VS-1, G-VS-2 and G-VS-3.

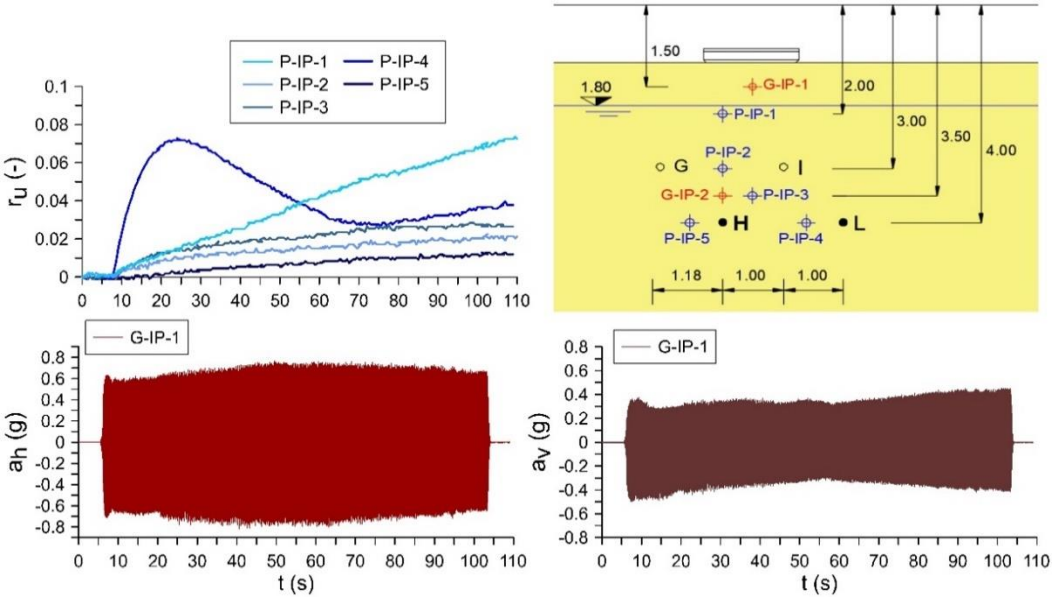

Figure 17. Results of test IPS_1. Time histories of: pore pressure ratio r_u; horizontal, a_h, and vertical, a_v, components of acceleration in the geophone G-IP-1. Geophone G-IP-2 did not work during the tests.

The settlement measured after the test IPS_1 was of 13 cm, of the same order of magnitude of the one measured after test UN_1. Since in this case there were no pore pressure increments and therefore no post cyclic consolidation, it is confirmed that the ruling displacing mechanism in this test was local densification below the loaded area.

6 CONCLUDING REMARKS

The liquefaction field trial tests carried out in Pieve di Cento with a shaker placed at ground level were able to induce significant pore pressure increments in the subsoil, locally generating liquefaction in one of the tests on the untreated soil.

The tests were also able to show the effectiveness of the mitigation measures implemented on site, and chosen among those studied in the LIQUEFACT project. For the sake of brevity, the paper does not show any result of the tests with HD, but it reports one of those carried out with IPS. The final value of the average degree of saturation was low enough to reduce pore pressure increments to negligible values. The huge amount of data retrieved from all the tests is now under detailed examination. Thus, the considerations reported in this paper are just preliminary.

ACKNOWLEDGMENTS

This work was carried out as part of the European project Horizon 2020 – Assessment and Mitigation of liquefaction potential across Europe: A holistic approach to protect structures infrastructures for improved resilience to earthquake – induced liquefaction disasters – "LIQUEFACT" (grant agreement No. 700748).

REFERENCE

Amoroso, S., Rollins, K. M., Lusvardi, C., Monaco, P. & Milana, G. 2018. Blast-Induced Liquefaction Results at the Silty-Sand Site of Mirabello, Emilia Romagna Region, Italy. *Geotechnical Earthquake Engineering and Soil Dynamics*, ASCE, 108–116.

van Ballegooy, S., Roberts, J. N., Stokoe, K. H., Cox, B. R., Wentz, F.J. & Hwang, S. 2015. Large-Scale Testing of Shallow Ground Improvements using Controlled Staged-Loading with T-Rex. *Proc. of the 6th ICEGE, Christchurch (New Zealand), 1-4 November 2015*.

Fasano, G., De Sarno, D., Bilotta, E. & Flora, A. 2018. Horizontal drains for the mitigation of liquefaction risk: design charts and experimental evidence. *Submitted for possible pubblication to Soils and Foundations*.

Fioravante, V., Giretti, D., Moglie, J., Bilotta, E., Flora, A., Fasano, G. & Nappa, V. 2019. Centrifuge modelling in liquefiable ground before and after the application of remediation techniques. *Proc. of the 7th ICEGE,* Rome, Italy.

Giretti, D. & Fioravante, V. 2017. Ruolo della geotecnica nella ricostruzione dopo il sisma dell'Emilia nel 2012. *Convegno Nazionale di Geotecnica*, AGI, Rome, 587–594.

Lirer, S., Bilotta, E., Chiaradonna, A., Fasano, G., Flora, A., Mele, L. & Nappa, V. 2019. Comparative analysis of soil liquefaction mitigation measures. *Proc. 17th ECSMGE, Reykjavik (Iceland), 1-6 September 2019*.

Mele, L., Lirer, S. & Flora, A. 2019. A liquefaction surface to describe liquefaction phenomena in unsaturated sandy soils. *Proc. of the 7th ICEGE,* Rome, Italy.

Mele, L., Tian, J. T., Lirer, S., Flora, A. & Koseki, J. 2018. Liquefaction resistance of unsaturated sands: experimental evidence and theoretical interpretation. *Géotechnique*. https://doi.org/10.1680/jgeot.18.P.042

Robertson, P. K. 2009. Interpretation of cone penetration tests — a unified approach. *Canadian Geotechnical Journal*, 46(11): 1337–1355.

De Sarno, D., Fasano, G., Bilotta, E. & Flora, A. 2019. Design method for horizontal drains in liquefiable soil. *Proc. of the 7th ICEGE,* Rome, Italy

Tamura, S., Tokimatsu, K., Abe, A. & Sato, M. 2002. Effects of Air Bubbles on B-Value and P-wave velocity of a partially saturated sand. *Soils and Foundations*. 42(1): 121–129